



RESEARCH ARTICLE

Kirkuk University Journal for Agricultural Sciences

ISSN:2958-6585

<https://kujas.uokirkuk.edu.iq>



<https://doi.org.10.58928/ku26.17127>

## Antimicrobial and Antioxidant Properties of Nanoparticles Synthesized From *Euphorbia* spp. extract in the Kurdistan Region of Iraq

Rozhiya Abdulljalil Nasr<sup>1</sup>

Shorish Mustafa Abdullah<sup>1</sup>

<sup>1</sup>Biology Department, Faculty of Science, Soran University, Erbil, Kurdistan region, IRAQ.

\*Corresponding Author: [rozhiya.nasr@soran.edu.iq](mailto:rozhiya.nasr@soran.edu.iq).

Received:27/10/2025

Revised: 28/11/2025

Accepted: 20/03/2026

Published: 29/03/2026

### ABSTRACT

This study was conducted to analyze the phytochemical composition of *Euphorbia* spp. extract using GC–MS and to evaluate its potential in the green synthesis of silver (Ag) and zinc oxide (ZnO) nanoparticles. The synthesized nanoparticles were further characterized by FTIR, XRD, SEM, and EDS analyses. For assessing antibacterial and antifungal activities, by well diffusion method. And DPPH assay was used for antioxidant activity for both plant extract and synthesized nanoparticles. The GC-MS analysis determined 23 phytochemicals, the major phytochemicals identified belonged to triterpenoid group including lupeol, lanosterol, and taraxasterol. Phytochemicals belong to other secondary metabolites were identified including phenols and alkaloids. These metabolites have major role as reducing and stabilizing agent in the process of nanoparticle formation, and mainly they control particle sizes and improve structural stability. SEM and XRD result showed that, AgNPs exhibited a uniform spherical morphology with strong crystallinity, while ZnONPs shows a moderate aggregation with shape variability. Regarding their antimicrobial activity, AgNPs shows higher antibacterial and antifungal activity compared to ZnONPs and plant extract. The DPPH assay test for *Euphorbia* plant extract shows potent antioxidant activity especially in high concentration. This study demonstrates a sustainable and successful green method for synthesizing biologically active nanoparticles, at the same time emphasizing *Euphorbia* spp. as abiogenic source as antioxidant and antimicrobial agent suitable for pharmaceutical and biomedicine applications.

**Keywords:** *Euphorbia* Spp., Phytochemical Profiling, Green Synthesis, Silver and Zinc nanoparticle, Antimicrobial Activity, Antioxidant Activity.

Copyright © 2026. This is an open-access article distributed under the Creative Commons Attribution License.

### INTRODUCTION

During recent years, Nanotechnology has emerged as a transformative field with applications spanning medicine, agriculture, and industry. Among various nanomaterials, silver (Ag) and zinc oxide (ZnO) nanoparticles have gained significant attention due to their antimicrobial and antioxidant properties [17,8]. While chemical and physical synthesis methods are commonly employed, green synthesis using plant extracts offers an eco-friendly, cost-effective alternative that produces biocompatible nanoparticles suitable for biomedical applications [5,4]. Among the methods practicing in creating nanoparticles the green synthesis method is the most preferred option due to its nontoxic nature for human and environment. Among the biological materials, plant phytochemicals are the main source used for green synthesis of nanoparticles, providing eco-friendly and biocompatible approaches that effectively reduce and stabilize nanoparticles while enhancing their biocompatibility for interaction with biological cells [6]. The Kurdistan region of Iraq, characterized by its diverse climate and rich biodiversity, harbors numerous medicinal plant species with unexplored potential for nanotechnology applications [48]. Among these, the genus *Euphorbia* (*Euphorbiaceae*) is particularly promising due to its documented phytochemical diversity, including terpenoids, flavonoids, and polyphenols, which exhibit various biological activities [34,22]. As an important source of different chemical compounds with specific structures and functions medicinal plants exhibit important biological activity such as antimicrobial, anticancer, antiviral, and antioxidant activities. At the same time those phytochemicals are responsible in the integration between nanotechnology and plant-based synthetic methods for metal nanoparticle production [14].

The genus *Euphorbia*, a member of the *Euphorbiaceae* family, is the third largest flowering plant family. *Euphorbia* spp. are widely distributed and can be found in all temperate and tropical regions, comprises about 300 genera and 8000 species [29]. Most belonging to *Euphorbia* genus are used in folk medicine in different parts of the world, especially in traditional Chinese medicine [35]. Previous studies reported the existence of wide range of phytochemicals in this genus including terpenoids, flavonoids and polyphenols [63], and triterpenoid, glycosides, diterpenoids [16]. These phytochemicals provide value to this genus in drug discovery as well as having different therapeutic applications such as cytotoxic, antitumor,

antibacterial, antiviral, and anti-inflammatory activities [63]. At the same time, some species belonging to *Euphorbia* genus are reported for their distinct toxic behavior and are highly skin-irritant, and these characteristics are return for having toxic, milky latex which plant uses naturally as a defense mechanism against herbivores [45]. The taxonomical feature of *Euphorbia spp* is an inflorescence structure called cyathium which is cuplike structure formed of connate bracts. This structure has a single stamen and single pistil with leaves like sepal and petal. The leaves arranged alternately, simple, oblong in shape and entire or smooth margins with glabrous surface and round apex. This species has a tap root system [31].

This study aims to investigate the phytochemical profile of selected *Euphorbia* species collected from the Soran District, Kurdistan Region, the genus *Euphorbia* was selected for this study due to its rich diversity of bioactive phytochemicals where limited scientific data are available despite their traditional medicinal use. and to utilize their aqueous extracts for the green synthesis of silver (Ag) and zinc oxide (ZnO) nanoparticles. In addition, the study seeks to evaluate the stability, efficiency, and biological activities of the synthesized nanoparticles, while highlighting the scientific and regional significance of these indigenous plant resources for future pharmacological applications, conservation efforts, and sustainable utilization. Scientifically, highlighting the region's rich botanical diversity. This study has the potential to open new pathways for therapeutic drug discovery based on indigenous plants.

## Materials And Method

### Study area and plant collection

The root parts of *Euphorbia spp* was collected from Rost village, Soran district, Erbil Provinces, located between 36°39.60 Latitude and 44°57.40 Longitude at the elevation 1103 m above sea level (Figure 1). The area is mountainous with a semi-arid climate. The soil type calcareous, generally gravelly, sandy with clay and brownish in color [18]. The field collection took place in 26 August 2024, when plants were in late vegetative and early flowering stage. A total of 25 healthy plants were randomly selected from different points across the site to ensure representative sampling. The root parts were collected manually using sterilized scissors and gloves to avoid contamination and collected manually and stored in cleaned labeled bags and transported to the lab for further processing (Figure 2). The collected samples were placed in sterilized, labeled bags and transported to the laboratory within 4 hours. Botanical references were used for plant identification based on morphological characteristics and the identification was confirmed by qualified botanists. The plant was taxonomically identified and authenticated at the Department of Biology Laboratory, College of Education, Salahaddin University Erbil, Kurdistan Region, Iraq, based on standard botanical keys and morphological characteristics. The identification was confirmed by qualified botanists, and a voucher specimen was deposited in the departmental herbarium for future reference.

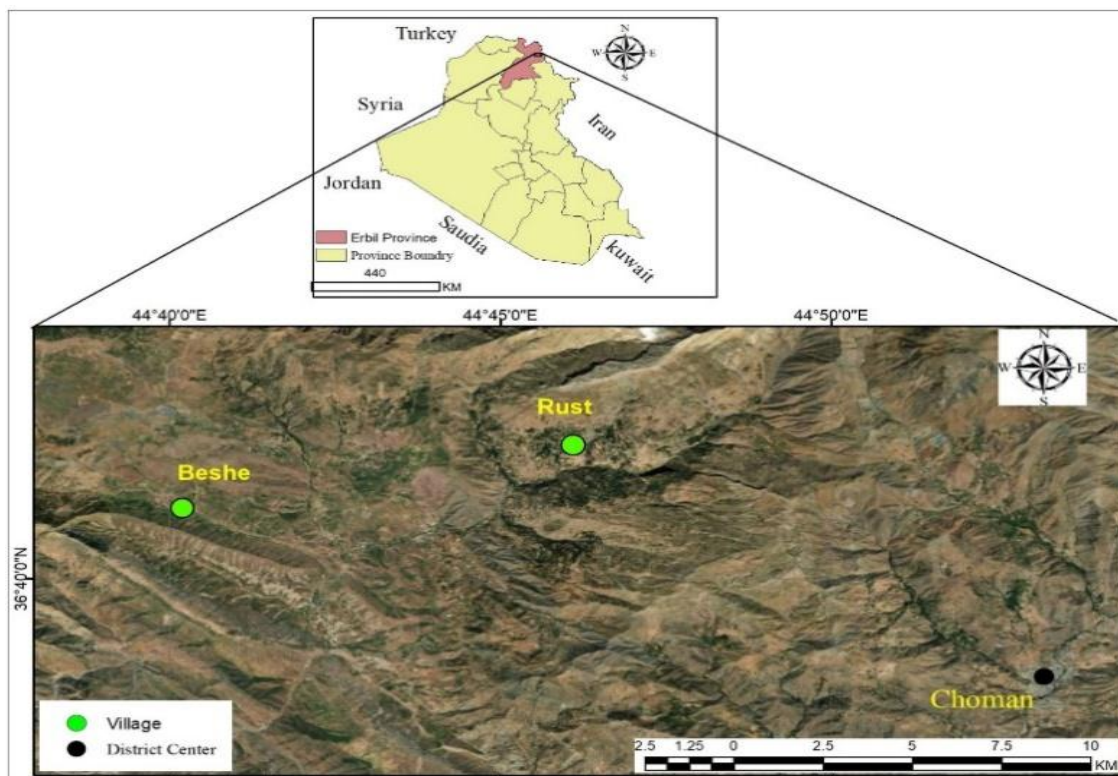


Figure 1. Location map of plant sample collection area



Figure 2. show *Euphorbia spp* collected in Rost valley in Soran district

## 2.2 Plant material preparation and extraction

The root parts of *Euphorbia spp.* were collected, carefully washed with tap water to remove dust and debris, and then shade-dried at room temperature ( $25 \pm 2^\circ\text{C}$ ) for 7–10 days the plant material was cut into small pieces and ground into a fine powder using an electrical mill (High speed multi-functional crusher, Model-200A, China) and stored in a container with a tightly closed lid until extraction. For antimicrobial activity testing and green synthesis of nanoparticles, distilled water was used to prepare aqueous plant extraction by using ultrasonic assisted extraction method. 5 g of powdered *Euphorbia spp* was mixed with 50 mL of distilled water in a ratio of 1:10 (w/v) and the mixture was placed in a conical flask and kept in an ultrasonic bath (Model Backer, Manufacturer, Sweden) for 30 min, at  $40^\circ\text{C}$  and 40 KHz frequency [64]. Then it was filtered using filter paper Whatman No. 41 [49]. For phytochemical profiling using GC-MS, ethanol was used for plant sample extraction due to its volatility and compatibility with the GC-MS system. The extraction procedure followed the exact same settings as the water-based extraction mentioned above [28].

## Synthesis of silver and zinc nanoparticles

Silver nanoparticles (AgNPs) and zinc oxide nanoparticles (ZnONPs) were synthesized using plant extract as a reducing and stabilizing agent. For AgNPs, 1 g of silver nitrate ( $\text{AgNO}_3$ ) was dissolved in 25 mL of distilled water, and 30 mL of plant extract was added to the solution. The pH was adjusted to 9 using 0.1 M NaOH added dropwise, and the mixture was stirred magnetically at 500 rpm for 30 minutes at  $60^\circ\text{C}$  to ensure homogeneity. The formation of AgNPs was indicated by a color change from yellow to deep brown. The residue was washed several times with distilled water and ethanol to remove impurities then dried at  $100^\circ\text{C}$  to remove residual water, and yielding and dried in an oven at  $100^\circ\text{C}$  for 1h. The final step in the synthesis was calcination, in which the dried powder was heated to  $400^\circ\text{C}$  for 30 minutes (Figure 3). The calcination process improves the crystallinity of the nanoparticles, making them suitable for various applications [43].

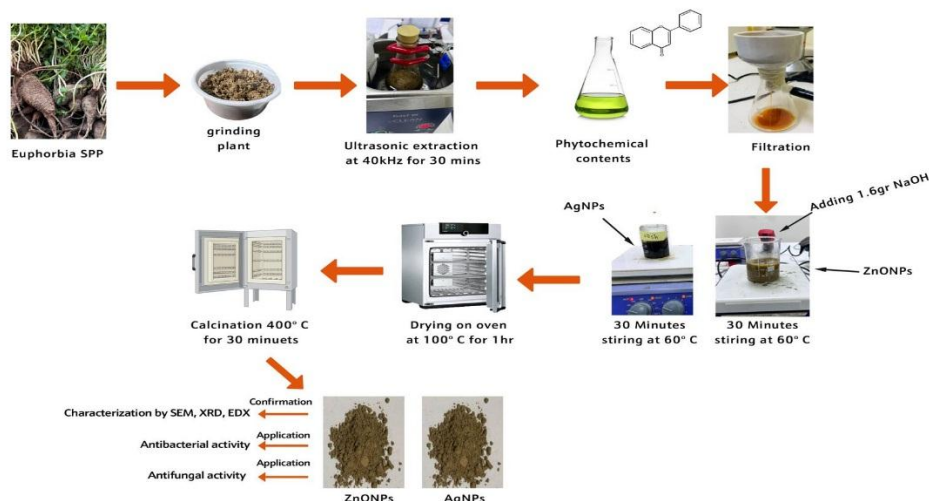


Figure 3. The synthesis of ZnONPs and AgNPs by using *Euphorbia spp*

## Antimicrobial activity evaluation

### Selection of Bacterial strains

The antibacterial activity of plant extract was tested against standard bacterial strains obtained from American Type Culture Collection (ATCC) including both gram-positive and Gram-negative bacteria. The Gram-positive species selected was *Staphylococcus aureus* (ATCC 25923), *Enterococcus faecalis* (ATCC 29212) and Gram-negative bacterial strains were *Proteus mirabilis* (ATCC 43071), *Salmonella bongori* (ATCC 13311), *Klebsiella pneumoniae* (ATCC13883), *Escherichia coli* (ATCC 29212) and *Shigella sp* (ATCC 9290) *Pseudomonas aeruginosa* (ATCC 27853). To ensure the identity and purity of the bacterial strains, several selective and differential tests were performed such as mannitol salt agar for the identification of *Staphylococcus aureus*, MacConkey agar for *Klebsiella pneumoniae*, *Escherichia coli*, and SS agar for *Shigella sp*, *Salmonella bongori* identifications and catalase test for *S. aureus* were performed for confirmation. [12].

### Isolation of fungal strains

For the evaluation of antifungal activity of *Euphorbia spp.* plant extract and green-synthesized AgNPs and ZnONPs, two fungal species were isolated from 30 urine samples obtained from patients at Helav hospital in Soran district Kurdistan Region, Iraq. Among these samples, 19 cases were candidiasis infections caused by fungi. The two isolated fungal species were identified as *Candida albicans* and *Candida tropicalis*. Following collection, samples were transported to the laboratory at 4 °C and processed within 2–4 hours. The samples were cultured on PDA plates and incubated for 72 h at 37 °C (Figure 4). *Candida albicans* was identified through microscopic observation by germ tube formation, while *Candida tropicalis* was confirmed based on colony coloration and morphology on CHROM agar medium [30]. The isolated fungi species were maintained on PDA to the time of conducting an antifungal assay against both plant extract and synthesized nanoparticles. for each treatment. Fluconazole served as the positive control.

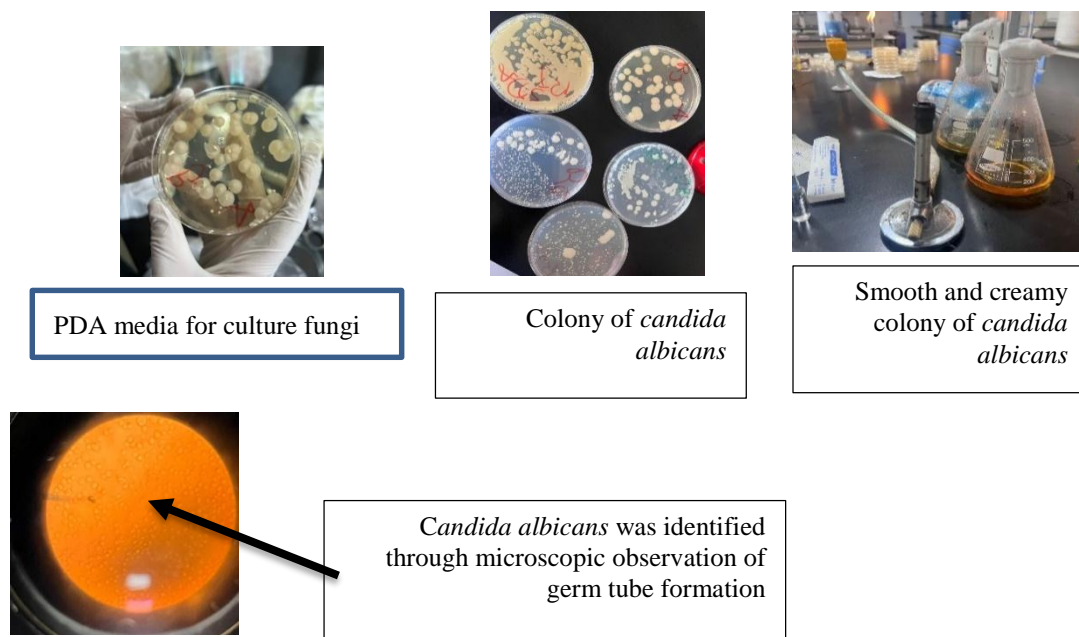


Figure 4. isolation of fungal species from urine samples

### Antimicrobial activity Assay

Antifungal and antibacterial activity of *Euphorbia spp.* extract and synthesized AgNPs and ZnONPs were evaluated using agar well diffusion method. Mueller-Hinton agar was used to perform antibacterial testing, while PDA was used to conduct antifungal testing. Overnight cultures of bacterial strains were grown in nutrient broth at 37°C. Bacterial suspensions were visually adjusted to a dense, homogeneous turbidity before plating. Agar Well Diffusion Procedure: Mueller-Hinton agar plates were poured to approximately 4 mm thickness. Wells of 8 mm diameter were made using a sterile cork borer, and 50 µL of each sample (*Euphorbia* extract, AgNPs, or ZnONPs) was added. Plates were incubated at 37°C for 24 h, and the diameters of inhibition zones were measured in millimeters using a digital caliper [47]. controls: CIP (10 µg/mL) served as the positive control for antibacterial activity. For antifungal activity, the experiment was conducted in the same setting of antibacterial testing except the fungal plates were incubated at 25 °C for 24 h used

Fluconazole (5 µg/mL).

#### Antioxidant activity assay

The antioxidant activity of *Euphorbia spp.* extracts was evaluated using the 2,2-diphenyl-1-picrylhydrazyl (DPPH) radical scavenging method. Plant extract stock solution was prepared by dissolving 10 mg of dried plant extract in 1 mL methanol. Serial dilutions were made to obtain final concentrations of 100, 50, and 10 µg/mL, with each solution vortexed to ensure complete mixing. Ascorbic acid was used as a standard and prepared in the same manner (10 mg in 10 mL methanol, diluted to 100, 50, and 10 µg/mL). A 0.1 mM DPPH solution was prepared in methanol. For the assay, 1 mL of DPPH solution was mixed with 1 mL of plant extract. The control consisted of 1 mL DPPH solution mixed with 1 mL methanol (without sample) to measure maximum absorbance. Methanol alone was used as a blank to zero the spectrophotometer. All mixtures were incubated in the dark at room temperature (~25 °C) for 30 minutes, with tubes covered in aluminum foil to prevent light-induced degradation. Absorbance was measured at 517 nm using a UV-Vis spectrophotometer [41].

The percentage of DPPH radical scavenging activity was calculated using the formula:

Antioxidant Activity (%) = [(A control – A sample) / A control] × 100  
A control = Absorbance of the control (without sample)

A sample = Absorbance in the presence of plant extract

Antioxidant Activity (%) = percentage DPPH radical that neutralized by antioxidant compounds present in the extract.

The calculated percentage represents the amount of DPPH free radicals neutralized by antioxidant compounds present in the plant extract.

### Instrumentation

#### GC–Mass analysis of plant *Euphorbia spp* extract

The ethanolic *Euphorbia spp* plant extract analyzed by GC-MS to identify phytochemical structure. The analysis was done using Agilent technologies GC system (7890B) coupled with Mass detector (5977) and automatic liquid sampler (7693A). HP-5MS capillary column (30m x 250 µm ID x 0.25 µm film thickness) was used for separation. The instrument was operated in (EI) mode at 70 eV. Helium gas in purity (99.995%) was used as carrier gas at a flow rate of 1 ml/min. The injection volume was 1 µl in split less mode. The injector temperature was set at 250 C and ion source temperature at 200 C. The oven temperature was programmed at 60 C isothermal for 2 minutes, then increased at a rate of 3 C/min to 150 C followed by 10 C/min to 300 C ending with 5 min isothermal at 300 C. Mass spectra data were acquired in the range of 45-550 m/z with a 0.5s scan interval. To avoid solvent interference, the solvent delay was set to 3 min. In our sequence, a blank sample consisting of the same solvent used for plant extraction was injected to detect any impurities that may exist in the solvent and at the same time to exclude them from the interpretation of the mass-spectral results. The achieved mass spectra were compared to the reference data from NIST (national institute of standard and technology) mass spectral library for identification the bioactive compounds.

#### Fourier transform infrared (FTIR) spectroscopy

To confirm successful formation and surface functionalization of the synthesized silver and zinc oxide nanoparticles, FTIR was employed. The analysis was conducted using Shimadzu IRspirite FTIR spectrophotometer equipped with the attenuated total reflectance (ATR) accessory. Dried synthesized nanoparticles were placed onto ATR without additional preparation. Spectra were recorded at 4000-400 cm<sup>-1</sup> at room temperature using a spectral resolution of 4 cm<sup>-1</sup> and the scan number was setup at 32 scan for each spectrum. In the same condition of the sample, background spectra was collected before each measurement and subtracted from the sample measurement. To confirm nanoparticles synthesis, absorption peaks corresponding to phytochemical group from plant extract should be presence as an indicator of reducing and capping ability in the nanoparticles.

#### Scanning Electron Microscopy (SEM)

To examine the surface morphology including particle shape, aggregation, surface texture and microstructural characteristics of the produced AgNPs and ZnONPs, field emission scanning electron microscope (FEI Quanta 450) was used. The SEM was operated at voltage 30 kV in high vacuum mode. Secondary electron detector (SED) under high vacuum was used to perform imaging.

#### Energy dispersive X-ray spectroscopy (EDS)

Bruker XFLASH 6/10 EDS microanalyzer was used to analyze the elemental composition of the synthesized nanoparticles. The EDS system was integrated with the SEM and featured an energy resolution of 121 eV at Mn Ka. The sample analysis was performed in both point and elemental mapping analysis to confirm the presence of Ag and Zn and verify the structure of the synthesized nanoparticles in both elemental composition and distribution.

#### Sputter coating

To maintain surface detail resolution during imaging, and before conducting SEM analysis, the samples were coated using Desk Sputter coating DSR1 from nano structured coating. Gold coating was selected and set the coating thickness to 30 nm (300 Å) with rotating applied to ensure uniform coating. The sputtering process was conducted at a coating current

of 20mA.

### UV-Visible Spectrophotometry

To evaluate the antioxidant activity of the plant extract using DPPH radical scavenging assay, Cecil-Super Aquarius dual-beam UV-Visible spectrophotometer was used. The absorbance measurements were recorded at 517nm [38].

## Results And Discussion

### 4.1 Phytochemical Profiling of *Euphorbia spp*

The GC-MS analysis of the *Euphorbia Spp.* Extract identified (23 compounds) (Table 1). The GC-MS chromatogram (Figure 5) shows distinct peaks corresponding to the various phytochemicals. Among the detected compounds, taraxasterol, lupeol, and lanosterol were the major compounds, with prominent peaks were observed at retention times of 57.636, 55.585, and 54.486 minutes, respectively.

Triterpenoids are known for their pharmacological activities, including anti-inflammatory, antimicrobial, antioxidant, and anticancer properties, highlighting the potential therapeutic applications of *Euphorbia spp* [37]. Taraxasterol, a pentacyclic triterpene, has been reported to exhibit anti-inflammatory, antibacterial and cytoprotective effects. Similarly, lupeol, an important triterpene, possesses anti-inflammatory, antioxidant, and antidiabetic activities, playing a crucial role in protecting cells from oxidative stress-induced damage. Lanosterol, a precursor compound in steroid biosynthesis is known for its pharmacological activities, including membrane stabilization and antioxidant defense [26].

Beyond their pharmacological relevance, the phytochemicals detected in *Euphorbia* root extract also play a critical role in green nanoparticle synthesis, functioning as both reducing and stabilizing (capping) agents that influence the size, shape, and homogeneity of the nanoparticles. Functional groups such as hydroxyl (-OH), carboxyl (-COOH), and other electron-donating moieties can reduce metal ions and simultaneously stabilize the resulting nanoparticles, preventing aggregation and enhancing stability [46]. In effect they have main role in the regulation process of nanoparticle size, shape and homogeneity. Phytochemicals such as phenols, sterols ( $\beta$ -sitosterol), and triterpenes (taraxasterol, lupeol, lanosterol) lupeol (55.585 min), lanosterol (54.486 min), and taraxasterol (57.636 min) as well as sterols such as  $\beta$ -sitosterol (53.739 min), were detected, indicating a high abundance of redox-active compounds capable of mediating nanoparticle formation. are among the effective phytochemicals because of their redox potential and surface binding ability [42]. Due to the presence of phytochemicals like flavonoids, diterpenes, and triterpenes, *Euphorbia* species perform similar functions and those phytochemicals support their applications environmentally friendly nanoparticle synthesis and facilitate the reduction of metal ions and stabilization of nanoparticles, highlighting their dual function in green synthesis [23]. The detection of some of these metabolites in the current *Euphorbia* plant extract could serve as a valuable natural source for nanomaterial production in a sustainable way.

Table (1): Phytochemical constituents of *Euphorbia Spp.* Extract detected by GC-MC

Hit No.	Hit name	Rt name	Peak Ara	Quality	CAS Number
1	Carbonyl-pi-Cyclopentadienyle-trichlorgemyl-cis-trimethylephosphan	4.906	258802	50	1000399-43-0
2	phenol, 4-[4,5-bis[4-(dimethylamino)phenyl]-1H-imidazol-2-yl]-2,6-dimethoxy-	5.234	273344	90	1000203-04-0
3	3,8,12-Tri-O-acetylingol 7-phenylacetate	9.267	68917	91	020071-49-2
4	1H-Cyclopropa[a]naphthalene, decahydro-1,1,3a-trimethyl-7-methylene-, [1aS-(1a.alpha.,3a.alpha.,7a.beta.,7b.alpha.)]-	10.427	273577	90	1000129-73-0
5	1-(2-d-Benzoyl-3,5-di-O-toluyyl-.beta.-d-ribofuranosyl)-5,6-dimethylbenzimidazole	13.15	273514	90	107579-33-9
6	7.alpha.,11.alpha.-Dihydroxytomatidine, O,O,O,N-tetraacetate	13.245	229219	45	345989-21-1
7	4-Allyl-5-(2,4-dichloro-phenyl)-2-morpholin-4-ylmethyl-2,4-dihydro-[1,2,4]triazole-3-thione	15.159	268092	80	036872-76-1
8	Lanost-9(11)-en-18-oic acid, 23-(acetyloxy)-3,20-dihydroxy-, .gamma.-lactone, (3.beta.,20.xi.)-	15.22	273980	70	070225-30-8
9	Nickel(II) bis(N,N-diheptyldithiocarbamate)	15.573	274623	71	1000225-76-5
10	2-(Dipropylamino)-4-[2,2,3,3,3-pentafluoro-1,1-bis(trifluoromethyl)propyl]-6-[2,2,2-trifluoro-1,1-bis(trifluoromethyl)ethyl]-1,3,5-triazine	16.972	241261	69	034062-84-5
11	Terephthalanilide, 4',4"-dinitro-	17.651	138642	72	005115-81-1

12	Desulphosinigrin	21.445	24544	40	081800-50-2
13	4,7,7-Trimethylbicyclo[4.1.0]hept-3-en-2-one	30.787	25410	84	065996-50-1
14	Pyrolo[3,2-d]pyrimidin-2,4(1H,3H)-dione	43.284	16874	73	043142-43-4
15	3,5-Nonadien-7-yn-2-ol, (E,E)-	50.589	245059	90	000083-46-5
16	.beta.-Sitosterol	53.739	245060	82	000083-47-6
17	.gamma.-Sitosterol	54.112	249535	58	000079-63-0
18	Lanosterol	54.486	249537	95	1000362-97-5
19	Tirucalol	54.662	249570	91	000469-38-5
20	9,19-Cyclolanost-24-en-3-ol, (3.beta.)-	54.961	249533	49	000545-47-1
21	Lupeol	55.585	254112	95	000511-61-5
22	9,19-Cyclolanost-25-en-3-ol, 24-methyl-, (3.beta.,24S)-	56.801	249541	70	001059-14-9
23	Taraxasterol	57.636	258802	56	1000399-43-0

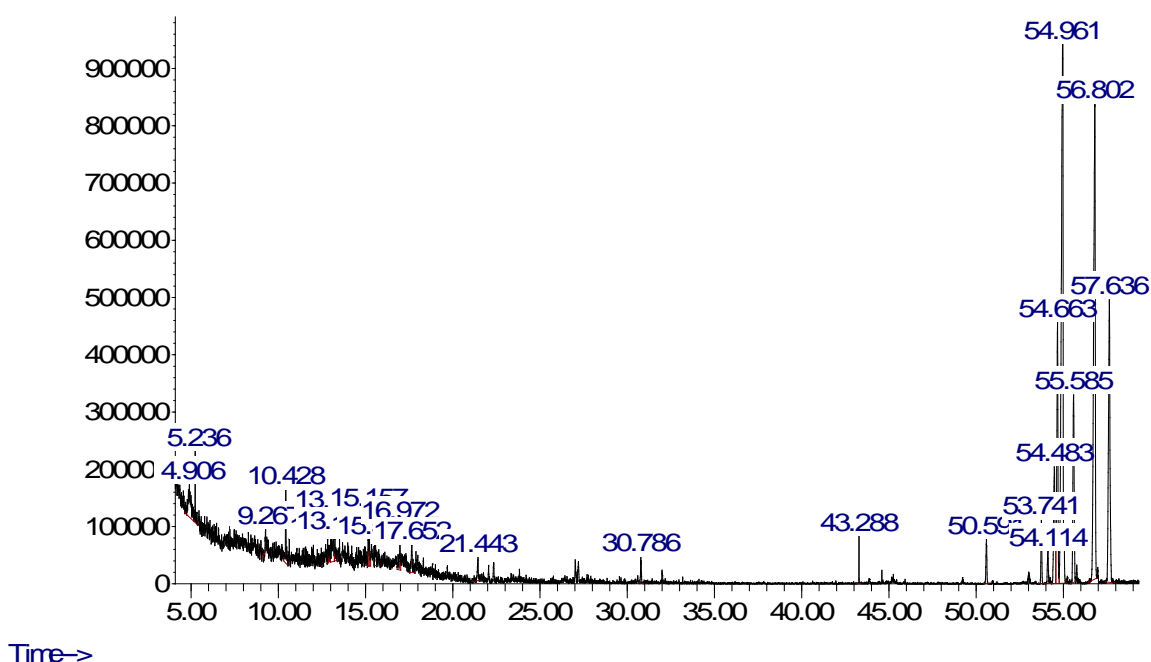


Figure 5. GC-MS chromatogram of ethanolic extract of *Euphorbia Spp*

### Green Synthesis and Characterization of Nanoparticle

The initial formation of silver (Ag) and zinc oxide (ZnO) nanoparticles was suggested by a visible color change upon adding the *Euphorbia* plant extract to the metal precursor solutions. The solution turned brown for AgNPs and milky white for ZnONPs, indicating the potential reduction of  $\text{Ag}^+$  and  $\text{Zn}^{2+}$  ions. However, visual observation alone is insufficient to confirm nanoparticle synthesis; therefore, further characterization using analytical techniques such as X-ray diffraction (XRD) patterns confirmed the crystalline nature of nanoparticles., Fourier-transform infrared spectroscopy (FTIR) analysis revealed functional groups associated with phytochemicals on the nanoparticle surface., and electron microscopy was performed to verify nanoparticle formation SEM images revealed predominantly spherical AgNPs with slight aggregation, while ZnONPs displayed irregular, quasi-spherical morphology, determine their physicochemical properties, and identify the role of specific phytochemicals in reduction and stabilization. EDS analysis confirmed elemental composition. 76.22% AgNPs contained 70% silver, with trace carbon and oxygen from capping phytochemicals, ZnONPs contained 48.76 % zinc.

### Fourier Transform Infrared (FT-IR)

The Fourier transform infrared (FTIR) analysis of the ZnO and AgNPs, as depicted in Figure (6), provides valuable insights into their chemical composition and interactions. A strong band peaks observed in plant extract at  $3328\text{ cm}^{-1}$  suggested O–H stretching vibrations of hydroxyl groups which are commonly found in phenolic compounds, alcohols, and flavonoids. These hydroxyl groups play a crucial role in reducing metal ions and stabilizing the formed nanoparticles as discussed before [62]. The absorption peak in plant extract at  $1700\text{ cm}^{-1}$  is characterized to C=O stretching vibration indicating the presence of amines or carboxyl coating biomolecules that effect the stabilization of nanoparticle [15]. Weaker

absorption bands in plant extract at  $1077\text{ cm}^{-1}$  and  $1150\text{ cm}^{-1}$  are indicated for C–O stretching vibrations associated with ethers or esters, which also participate in nanoparticle capping. The peak in plant extract at  $1457\text{ cm}^{-1}$  corresponds to C=C stretching vibrations, likely characteristic of phenolic compound known as strong reducing agents [39].

A broad absorption band observed in AgNPs at  $3300\text{ cm}^{-1}$  corresponds to O–H stretching vibrations of hydroxyl groups, commonly present in phenolic compounds, flavonoids, and alcohols. These groups act as reducing agents for  $\text{Ag}^+$  ions and as capping agents, preventing aggregation and controlling particle size [19]. These functional groups reveal the participation of bioactive compounds from Euphorbia plant extract as reducing, capping, and stabilizing agents in the nanoparticle formation process [52]. Similar to AgNPs, a broad O–H stretching band appears in ZnONPs at  $3300\text{--}3325\text{ cm}^{-1}$ , confirming participation of hydroxyl-containing phytochemicals in the reduction of  $\text{Zn}^{2+}$  ions, the reduction bands from  $3328\text{ cm}^{-1}$  to  $3300$  and along present peak at  $500\text{ cm}^{-1}$  is further confirm the bio reduction of  $\text{Ag}^+$  ions to  $\text{Ag}^0$  and  $\text{Zn}^{+2}$  to  $\text{ZnO}$  [15]. In general, The FTIR results show that the dual functionality of Euphorbia plant phytochemicals has a major role in green synthesis of nanoparticles through providing reduction and stabilization characterization to the reactions. This eco-friendly biosynthesis process excludes the necessity of using hazardous chemicals in the production process and produces nanoparticles with potential applications in medicine [2].

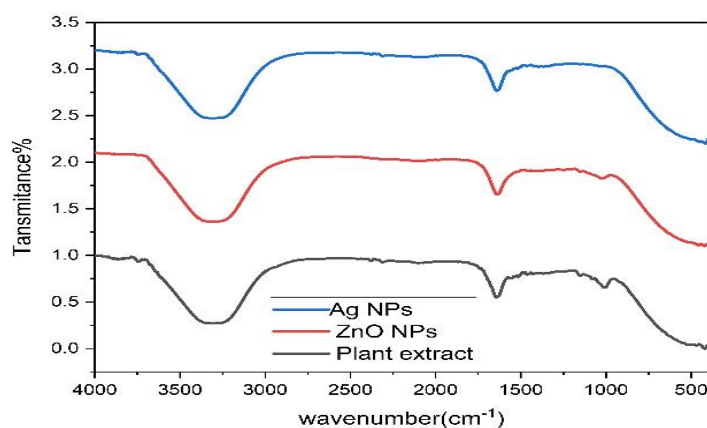
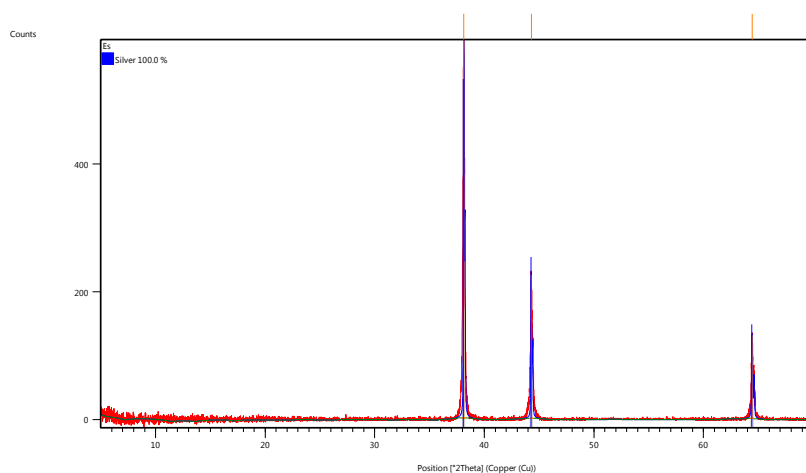


Figure 6. FTIR analysis of *Euphorbia spp* extract ,AgNPs and ZnONPs showing characteristic functional groups participated in the formation of nanoparticle.

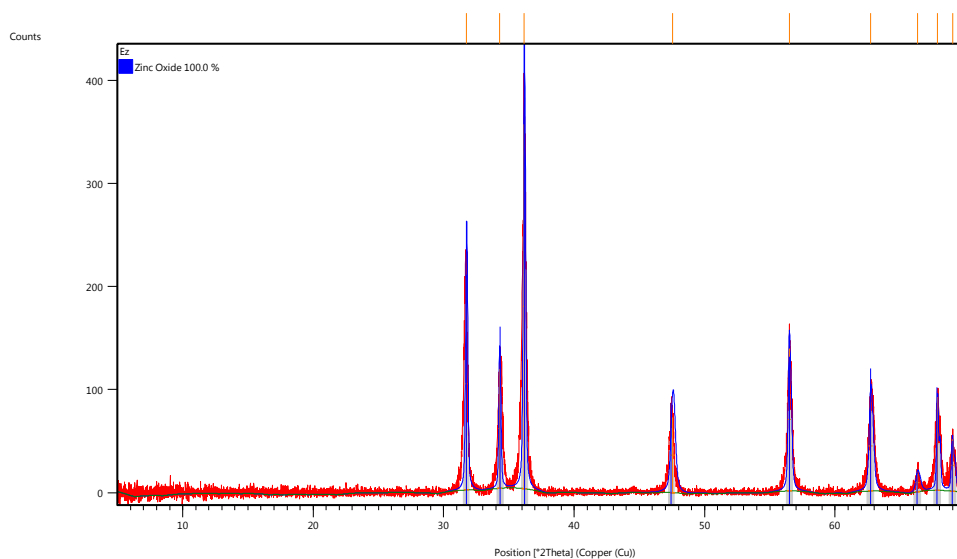
### X-ray diffraction (XRD)

The X-ray diffraction (XRD) patterns of the synthesized results AgNPs and ZnONPs are presented in Figure (7) and (8). The diffraction peaks observed for silver nanoparticles at  $2\theta$  values of  $38.13^\circ$ ,  $44.28^\circ$ , and  $64.43^\circ$  match to the 111, 200, and 220 crystallographic planes of silver face centered cubic with ICSD database (reference 98-005-3761). Similarly, the diffraction peaks of zinc oxide (ZnO) which appear at  $2\theta$  positions ( $2\theta$ ) of  $31.74^\circ$ ,  $34.28^\circ$ ,  $36.16^\circ$ , and  $47.5573^\circ$  are the peaks corresponding to the 100, 002, 101, and 102 crystallographic planes of hexagonal wurtzite zinc oxide (ZnO) (reference 98-065-6331), [51] These result confirms the formation of crystalline Ag and ZnO nanoparticles successfully. The absence of amorphous peaks in the XRD patterns supports the formation of highly crystalline ZnO and Ag nanoparticles [10]. Crystallinity is a critical attribute that influences the nanoparticles' functional properties, including their antioxidant and antimicrobial activities, as reported in previous studies [33]. Overall, the diffraction peaks are characterized by sharp and well-defined peaks reflecting high structural order and uniformity, confirming the effectiveness of the used green synthesized method.



Visible	Ref. Code	Score	Compound Name	Displacement [°2Th.]	Scale Factor	Chemical Formula
*	98-005-3761	88	Silver	0.000	0.891	Ag1

Figure 7. XRD pattern of AgNPs synthesized using *Euphorbia spp.* extract



Visible	Ref. Code	Score	Compound Name	Displacement [°2Th.]	Scale Factor	Chemical Formula
*	98-065-6331	86	Zinc Oxide	0.000	0.870	O1 Zn1

Figure 8. XRD pattern of ZnONPs, synthesized using *Euphorbia spp.* extract

### Scanning Electron Microscopy

The scanning electron microscopy (SEM) images presented provide a detailed insight into the morphological characteristics of the prepared AgNPs and ZnONPs (Figure 9 & 10). These images were captured at various magnifications to examine the surface morphology including, particle shape, aggregation, surface texture and microstructural characteristics nanoparticles.

The SEM images of AgNPs showed the spherical and uniformly distributed particles with the size of 100 to 200 nm (Figure 9) The morphology of the surface looks dense with minimal aggregation and well ordered, this indicating that the secondary metabolites in the *Euphorbia* extract acted as stabilizing and capping agents during synthesis effectively. The uniform spherical shape and particle size distribution indicate that the nucleation process and surface stabilization occurred in a

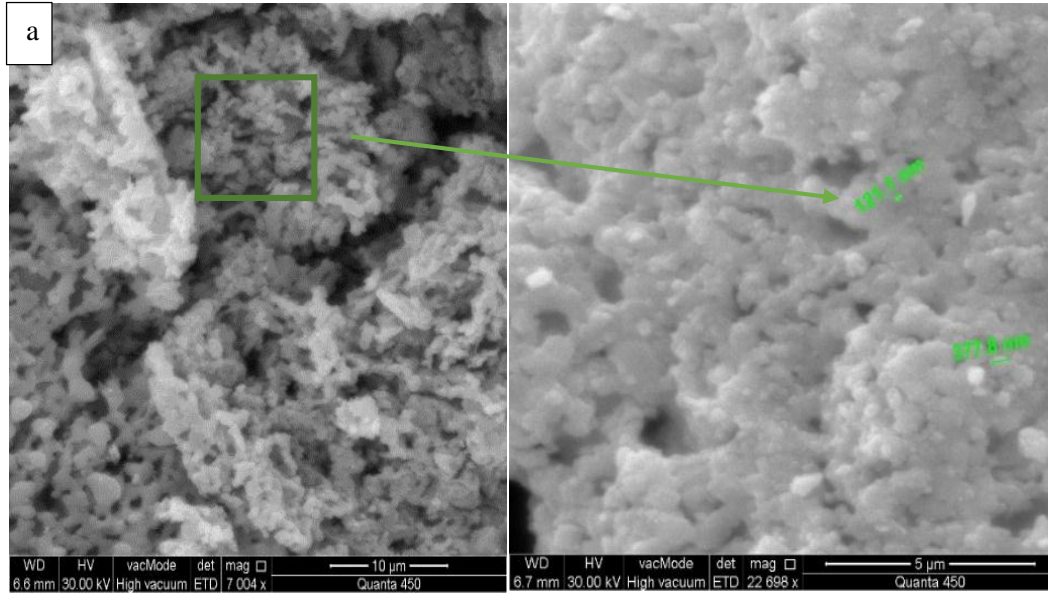


Figure 9. Scanning electron microscopy (SEM) image of silver nanoparticle synthesized using *Euphorbia spp.* Extract

controlled manner, reflecting the efficiency of the green synthesis of nanoparticles.

In contrast, the SEM image of ZnONPs Figure (10) shows a mixture of spherical shapes with heterogeneous size distribution, irregular shape, and rough surface, with particle size between 150 to 250 nm. The irregular shape impacts the chemical and physical properties of this nanoparticle. Partial agglomerations observed in ZnONPs, may associated to large surface area, irregular shape, rough surface and non-uniform nucleation during synthesis, which promote particle-particle interactions. This phenomenon is a common feature of metal oxide nanoparticle synthesized using plant secondary metabolites due to the composition of the organic matrix and differences in the precursor reactivity.

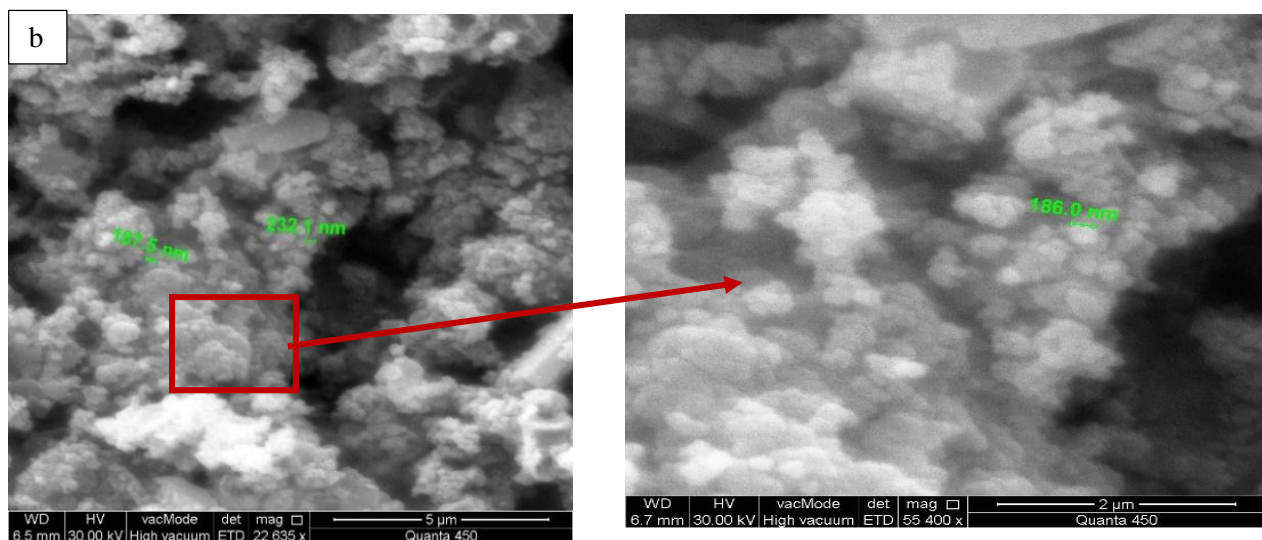


Figure 10. Scanning electron microscopy (SEM) image of ZnONPs synthesized using *Euphorbia spp.* Extract

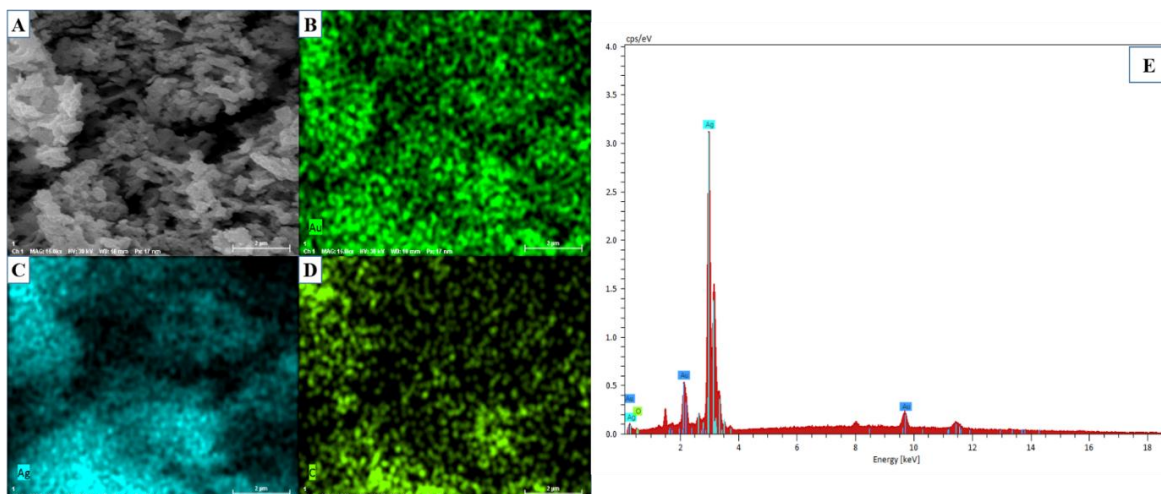


Figure 11. Energy dispersive X-ray spectroscopy (EDS) spectrum of silver nanoparticle (AgNPs) formed using *Euphorbia* extract and coated with gold. The EDS spectrum displaying the elemental composition of the mapped region, the prominent peaks corresponding to 76.22% silver (Ag) with minor peaks of gold (Au), 23.78% oxygen

The morphological differences between silver and zinc nanoparticles demonstrate that there are differences between the two metals in synthesis mechanism and growth kinetics. AgNPs are characterized by smoother surface and more homogeneous, while ZnONPs exhibit more irregularity. These differences in structure have effect on the chemical and biological properties of the synthesized nanoparticles. Spherical nanoparticles with smaller in size are more effective for many applications due to higher surface reactivity [57]. The smaller particle size of nanoparticle in this study may be due to the presence of the high concentration of hydroxyl and phenolic groups in *Euphorbia* extract which they act as stabilizing agents and prevent aggregation [50]. Furthermore, spherical nanoparticles have been reported to have more cellular uptake than rod-like shapes nanoparticles and are more effective for different biological applications. This difference explains why microorganism tend to be more sensitive to AgNPs than ZnONPs. [21].

#### Energy- Dispersive Spectroscopy (EDS) Analysis of silver and zinc nanoparticles

The energy-dispersive X-ray spectroscopy (EDS) analysis was conducted to find out the elemental composition of produced AgNPs and ZnONPs (Figure 11 & 12). This analysis is essential for understanding essential qualitative and quantitative information about the elemental composition of the synthesized ZnO and Ag nanoparticle and confirming the purity of the elements and participating the phytochemical compounds from the *Euphorbia* extract in the formation of nanoparticles.

The EDS spectrum of AgNPs (Figure 11). The EDS spectrum Figure 7 provides details of the elemental composition, silver element that the dominant element identified was approximately 76.22%, additionally, minor peaks of 23.78% oxygen, 2.33% copper, and gold were present in small amounts. The presence of gold is attributed to the gold coating applied to the samples to enhance SEM imaging conductivity and resolution [43]. The copper peak comes from the Cu tape that was used for mounting the nanoparticle samples on the sample holder. Regarding the oxygen peak, it may originate from oxygen-containing functional groups (-C=O, -COOH, -OH) of the plant extracted phytochemicals which act as capping agent and create a thin surface oxide layer [58]. The high silver content and purity verify the process of reduction of  $\text{Ag}^+$  to  $\text{Ag}^0$  successfully, and supporting the production of stable Ag nanoparticles effective and suitable for biological applications like antibacterial and antifungal activity [20].

In the case of ZnONPs showed in Figure (12) In the case of ZnONPs showed in Figure 8 elemental composition of ZnONPs the zinc element dominant element identified was approximately 48.76% of the composition. Other elements detected such as % 2.77 copper, % 40.22 oxygen. The presence of carbon is due to phytochemical present in the plant extract acting as capping and stabilizing agents during synthesis. [55]. These results confirm the successful biosynthesis of high-purity ZnO nanoparticles with the existence of bio-organic metabolites involving particle stabilization. Overall, the EDS results confirm the successful biosynthesis of high-purity Ag and ZnO nanoparticles with dominant metallic structure. The elemental composition supports the green synthesis of nanoparticle using *Euphorbia* plant extract, with a high content of desired metals and the presence of capping agents [54].

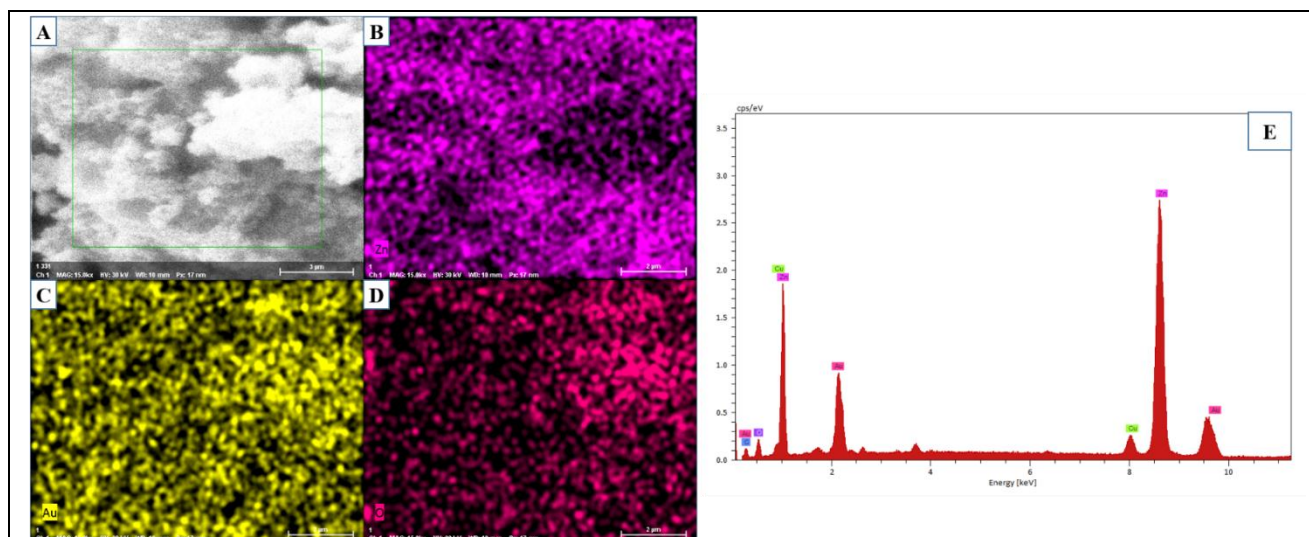


Figure 12. Energy dispersive X-ray spectroscopy (EDS) spectrum EDX result of zinc nanoparticle (ZnONPs) formed using *Euphorbia* extract and coated with gold Clusters of micron-sized minerals with distinct geometric morphologies are observed in silver nanoparticle, by SEM image show EDX elemental map highlighting zinc (Zn) distribution also oxygen and gold detected.(E)The EDX spectrum displaying the elemental composition of the mapped region, the prominent the prominent peaks corresponding to 48.76% zinc (Zn) with minor other peaks of are carbon gold (Au), and 40.2% oxygen (O), and 2.77% copper (Cu)

#### Antibacterial activity

In the present study, different gram-positive and gram-negative bacteria were used to screen the possible antimicrobial activities of *Euphorbia* spp., green synthesized silver (AgNPs) and zinc oxide (ZnONPs) nanoparticles against bacterial strains including *Staphylococcus aureus*, *E.coli*, *Salmonella bongori*, *Shigella spi.*, *Proteus mirabilis*, *Klebsiella pneumoniae*, *Pseudomonas aeruginosa*, and *Enterococcus faecali*. The results are summarized in (Table 2).

Table (2) :Antibacterial activity of *Euphorbia* spp. extract, silver nanoparticle (AgNPs), zinc oxide nanoparticle (ZnONPs) and antibiotic CIP10 as positive control

Microorganism	Silver nanoparticle(mm)	Zinc nanoparticle (mm)	Extract (mm)	Antibiotic CIP10 (mm)
<i>E.coli</i>	35	5	0	40
<i>Staphylococcus aureus</i>	33	0	0	35
<i>Salmonella bongori</i>	35	20	0	30
<i>Shigella sp.</i>	47	4	0	34
<i>Klebsiella pneumoniae</i>	46	3	0	40
<i>Protues mirabilis.</i>	39	0	0	35
<i>Pseudomonas aeruginosa</i>	36	12	0	40
<i>Enterococcus faecali</i>	34	0	0	36

Green synthesis of silver nanoparticles shows strong antimicrobial activity against all bacteria species (Figure 13). The highest inhibition zones were observed against Gram-negative bacteria, with *Shigella sp.* showing zone (47 mm), *Klebsiella pneumoniae* (46 mm), *Proteus mirabilis.* (39 mm), *Pseudomonas aeruginosa.* (36 mm). *Salmonella sp* and *E. coli sp.* both showed an inhibition zones of (35 mm), while the lowest inhibition zone observed for *Staphylococcus sp.* and *Enterococcus faecali.* with inhibition zone (33 mm) and (34 mm) respectively.

In contrast, green synthesized of zinc oxide nanoparticles (ZnONPs) have limited antibacterial activity, with inhibition zones ranging from (3 mm) to (20 mm) (Table 2). The highest antimicrobial activity recorded was against *Salmonella bongori* (20 mm), followed by *Pseudomonas aeruginosa* (12 mm). The *Euphorbia* spp extract alone has no significant antibacterial activity against any tested bacteria species (Figure 14). This may be due to the extraction process. Probably because of the degradation of thermolabile secondary metabolites during ultrasound-assisted extraction process. Although ultrasound-assisted extraction reducing extraction time but the temperature may degrade the phytochemicals, by producing free radical, the higher sensitivity of Gram-negative bacteria may be attributed to their thinner peptidoglycan layer and

outer membrane, which facilitates the penetration of AgNPs into the cell, leading to disruption of membrane integrity and intracellular damage. In contrast, Gram-positive bacteria possess a thicker peptidoglycan layer, which acts as a partial barrier against nanoparticle penetration, resulting in comparatively lower inhibition zones [36].

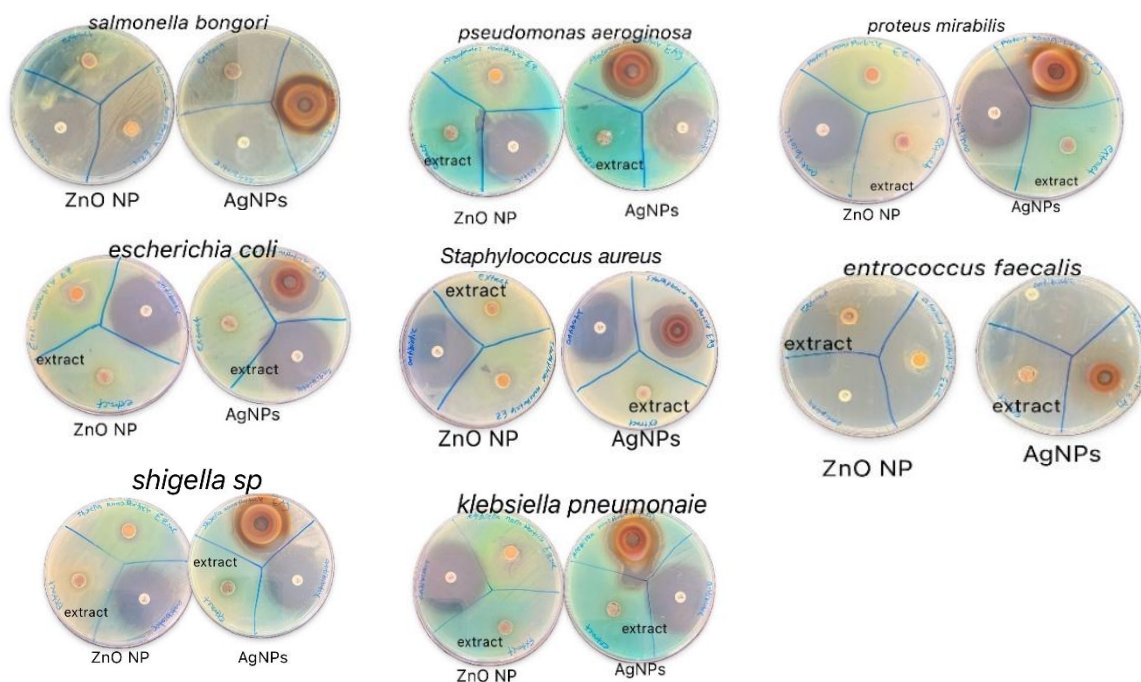


Figure 13. Antibacterial activity of *Euphorbia* spp. extract, silver nanoparticles (AgNPs), and zinc oxide nanoparticles (ZnONPs) against tested bacterial species, with CIP10a as a positive control.

Silver nanoparticles (AgNPs) demonstrated the most effective and strong antibacterial activity then both zinc nanoparticles and plant (Figure 13). This is likely due to their small particle size and uniform spherical shape, as confirmed by SEM. Smaller particles with larger surface area leads of enhancing interaction with bacterial cell membranes, which causes structural disruption and releasing cellular contents [11]. The result shows that, the Gram-negative bacteria are more sensitive to AgNPs compared to Gram positive strains, and this is because of their thinner cell membrane (thinner peptidoglycan layer), and the existence of lipopolysaccharides (LPS) which are negatively charged and promote nanoparticle binding [13]. Silver nanoparticle antibacterial action are reported to be happening in multiple mechanism, starting from interaction with cell wall, destroying the membrane, generate reactive oxygen species (ROS), and disrupting of the hydrogen bonding between DNA base pairs and interference with protein function [53].

Zinc oxide nanoparticles (ZnONPs) though less effect, also have antibacterial characteristics. Its action mostly related to generation of reaction oxygen species (ROS) [44]. Reactive oxygen species enhanced ZnONPs against bacteria under UV exposure, and generate superoxide anion ( $O_2^-$ ), hydrogen peroxide ( $H_2O_2$ ), and hydroxide ( $OH$ ). All of them that toxic for bacteria and cause damage to cell membrane, DNA, and proteins [24]. zinc nanoparticle less effect on Gram-positive bacteria due to present thick layer of peptidoglycan which affect the penetration of nanoparticles negatively [3], whereas Gram-negative bacteria are vulnerable more because of weaker cell wall and the existence of teichoic and lipoteichoic acid in the peptidoglycan layer that enhance the interaction of ZnONPs with the membranes [7].

Fungal species	Silver nanoparticle	Zinc nanoparticle	Extract	fluconazole
<i>C. albicans</i>	40mm	20mm	7mm	5mm
<i>C tropicalis</i>	30mm	15mm	15mm	5mm

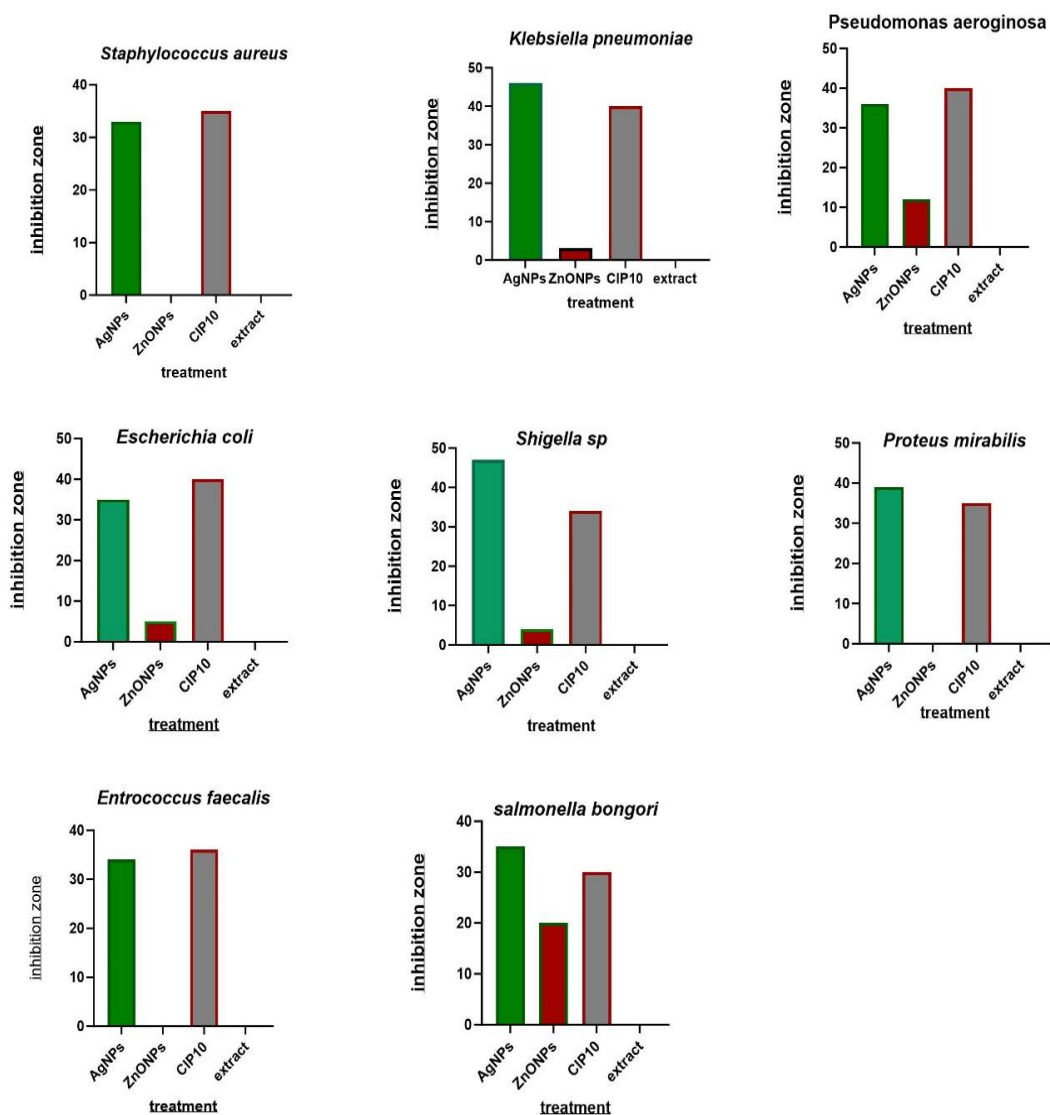


Figure 14. The figure illustrates the antibacterial activity of AgNPs, ZnONPs, ciprofloxacin (CIP) and *Euphorbia spp.* extract against different bacterial strains

### Antifungal activity

The antifungal activity of *Euphorbia spp.* plant extract and nanoparticles (silver and zinc) was evaluated against two fungal species: *candida albicans* and *candida tropicalis* with results summarized in table (3). AgNPs showed strong antifungal activity against both species, with highest inhibition zone (40 mm) against *C. albicans* and (30 mm) against *C. tropicalis*. ZnONPs exhibited moderate antifungal activity, with inhibition zones (20 mm) against *C. albicans* and (15 mm) against *C. tropicalis*. Although ZnONPs show antifungal effects, their activity was weaker than AgNPs (Figure 15 & 16).

Table (3) Antifungal activity of *Euphorbia spp.* silver nanoparticle (AgNPs), zinc oxide nanoparticle (ZnONPs) compared to fluconazole

The fungal cell wall, composed primarily of glucans, chitin, mannoproteins which are acritical factors in resistance against antifungal agents [27]. Both *C. albicans* and *C.tropicalis* were sensitive to both type of nanoparticles mostly because of damaging of cell wall and membrane as a result of membrane-nanoparticle interaction [56].

Silver nanoparticles (AgNPs) have significant antifungal role by different mechanisms including damaging cell wall and membrane, formation pore membrane leading to ion leakage and cellular distraction [14]. Additionally, they also induce vacuole formation and generate reactive oxygen species (ROS) that cause damage DNA, lipids and protein [40]. Silver nanoparticles (AgNPs) can affect fungal metabolism including biogenesis of mycotoxin (deoxynivalenol) and change synthesis of secondary metabolism in fungi [32]

Zinc oxide nanoparticles (ZnONPs) have been reported its effectivity against *C. albicans* which reduce fungal activity and distraction of cell wall component such as glycoproteins, polysaccharides glucan and chitin hydrophobics, and amphipathic proteins [38]. Their antifungal activity also includes inhibition enzyme activities, DNA damage, and inactivation of protein [37].

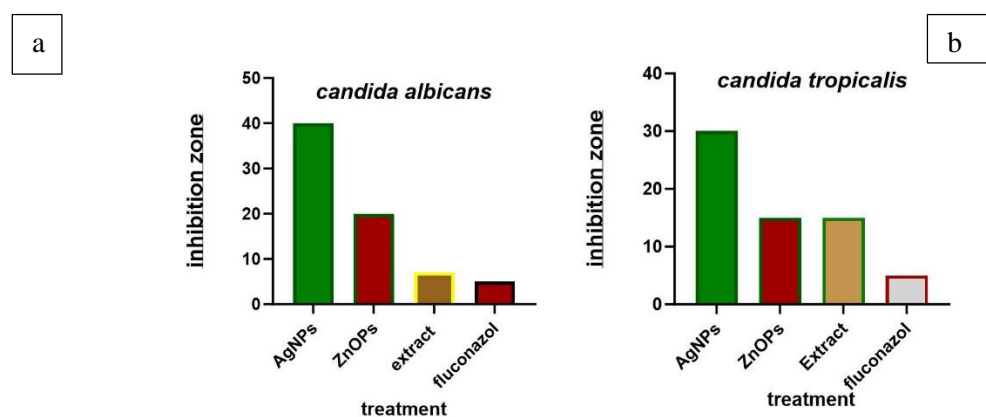


Figure 15. The figure illustrates the antifungal activity of AgNPs, ZnONPs, *Euphorbia spp.* extract and fluconazole against different fungal species

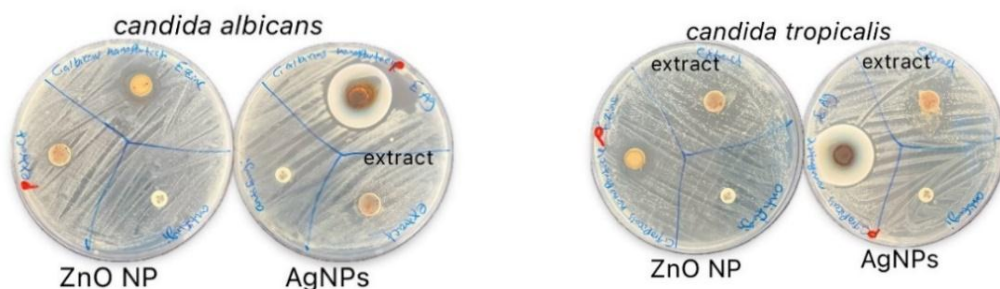


Figure 16. Antifungal activity of *Euphorbia spp.* extract, silver nanoparticle (AgNPs), zinc oxide nanoparticle (ZnONPs) and antifungal fluconazole, showing inhibition zone against *Candida albicans* and *Candida tropicalis*

#### Antioxidant activity

The antioxidant activity of *Euphorbia spp.* was evaluated using 2,2-diphenyl-1-picrylhydrazyl (DPPH) radical scavenging assay at three concentrations (100, 50, and 10  $\mu\text{g/mL}$ ), and the results were compared with ascorbic acid as the standard reference antioxidant. Plant concentration at 100  $\mu\text{g/mL}$  achieved the highest radical scavenging activity with an inhibition percentage of approximately 85%, compared to standard ascorbic acid inhibition which was near to 90%. The second radical scavenging activity was observed in plant extract with concentration 50  $\mu\text{g/mL}$  exhibited 83% inhibition, while at 10  $\mu\text{g/mL}$  exhibited 40% (Figure 17).

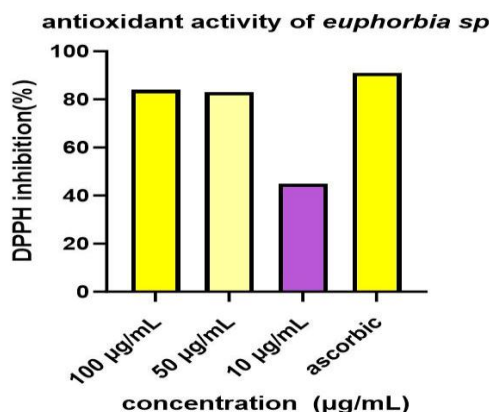


Figure 17. Antioxidant activity of *Euphorbia spp.* extract at different concentrations (100, 50, and 10 µg/mL). use of DPPH as radical scavenging activity, highest inhibition recorded at 100 µg/mL around 85%, also at 50 µg/mL 83%, but at a concentration of 10 µg/mL, the extract exhibited lower radical scavenging activity with ascorbic acid as a standard.

These antioxidant effects are visually confirmed by the change in color from purple to yellow shown in (Figure 18), which reflect the reduction of the stable DPPH radical through hydrogen atom or electron donation from bioactive compounds in the plant extract [26]. This visual observation was supported by the quantitative DPPH assay results, which showed a concentration-dependent increase in radical scavenging activity, with the highest inhibition percentage recorded at the maximum tested concentration. Ascorbic acid was used as a positive control, while DPPH solution without extract served as the negative control, ensuring the reliability and comparability of the results. These findings confirm that *Euphorbia* secondary metabolites act as effective electron donors, stabilizing reactive oxygen species by converting them into non-reactive forms, thereby demonstrating their significant antioxidant potential.

According to these results, *Euphorbia spp.* has strong antioxidant potential, especially at higher concentration. This is due to the presence of phenolic compounds, flavonoids, or other secondary metabolites, which are known to have the ability to neutralize oxidative stress by scavenging free radicals [42].



Figure 18. Antioxidant activity of *Euphorbia spp.* using the DPPH free radical scavenging assay at different concentrations (100, 50, and 10 µg/mL): strong antioxidant activity of *Euphorbia spp.* observed at 100 and 50 µg/mL, changing color from purple to yellow, but at 10 µg/mL the extract exhibited lower radical scavenging activity with ascorbic acid as a standard.

## Conclusion

This study successfully achieved the green synthesis of silver nanoparticles (AgNPs) and zinc oxide nanoparticles (ZnONPs) using *Euphorbia spp.* root extract as an efficient reducing and stabilizing agent. The presence of key secondary metabolites—particularly phenolics and flavonoids—played a critical role in the bioreduction and capping processes, as confirmed through FTIR, GC–MS, SEM, EDS, and XRD analyses. These findings align with previous studies reporting the involvement of plant-derived biomolecules in nanoparticle formation and stabilization, further validating the suitability of *Euphorbia* species for green nanotechnology applications.

Overall, the results highlight *Euphorbia spp.* as a promising, eco-friendly, and sustainable source for the fabrication of bio-functional nanoparticles with strong antimicrobial and antioxidant properties. Future research should focus on isolating specific phytochemicals responsible for nanoparticle formation, optimizing synthesis parameters to improve stability and yield, and conducting in vivo toxicity and efficacy studies to pave the way for biomedical, pharmaceutical, and environmental applications.

## Acknowledgments

### In the name of Allah, the Most Merciful and Compassionate

This study was conducted in the Feld of the College of biology, University of soran, Iraq. Great thanks to the staff in these Feld for providing the equipment, requirements, and facilities. I would like to offer my sincerest gratitude and appreciation to my supervisor, Dr. Shorsh Mustafa Abdulla for his supervision of my thesis project, for his teaching and continuous guidance of my way towards scientific research, which was of great support throughout all of my research work and thesis preparations. This study was conducted in the Feld of the College of biology, University of Soran, Iraq. Great thanks to the staff in these Feld for providing the equipment, requirements, and facilities

## Conflict of Interest

The authors declare that there are no conflicts of interest regarding the publication and/or funding of this manuscript

## References

- [1]. Abdullan, A. O., & Balaky, S. M. (2022). Stratigraphy and mineralogy of Balambo Formation (Aptian–Cenomanian) near Chomabrok village, Imbrication Zone, Iraqi Kurdistan Region. *Tikrit Journal of Pure Science*, 27(5), 57–67. <https://doi.org/10.25130/tjps.v27i5.18>
- [2]. Abdullah, F. O., Hussain, F. H., Sardar, A. S., Gilardoni, G., Thu, Z. M., & Vidari, G. (2022). Bio-active compounds from *Teucrium* plants used in the traditional medicine of Kurdistan Region, Iraq. *Molecules*, 27(10), 3116. <https://doi.org/10.3390/molecules27103116>
- [3]. Adeyemi, J. O., Oriola, A. O., Onwudiwe, D. C., & Oyedeji, A. O. (2022). Plant extract-mediated metal-based nanoparticles: Synthesis and biological applications. *Biomolecules*, 12(5), 627. <https://doi.org/10.3390/biom12050627>
- [4]. Ajiboye, B., Ibukun, E., Edobor, G., Ojo, A., & Onikanni, S. (2013). Chemical composition of *Senecio bialrae* leaf. *Scientific Journal of Biological Sciences*, 2(8), 152–159. Retrieved November 22, 2025, from [https://www.academia.edu/download/52508857/Chemical\\_composition\\_of\\_Senecio\\_bialrae\\_20170406-6389-5y6go2.pdf](https://www.academia.edu/download/52508857/Chemical_composition_of_Senecio_bialrae_20170406-6389-5y6go2.pdf)
- [5]. Alahmdi, M. I., et al. (2022). In vitro anticancer and antibacterial activity of green synthesized ZnO nanoparticles using *Clitoria ternatea* flower extract: Inhibits MCF-7 cell proliferation via intrinsic apoptotic pathway [Preprint]. *Research Square*. <https://doi.org/10.21203/rs.3.rs-1269775/v1>
- [6]. Alshamsi, H. A. H., & Hussein, B. S. (2018). Hydrothermal preparation of silver-doped zinc oxide nanoparticles: Characterization and photocatalytic activity. *Oriental Journal of Chemistry*, 34(4), 1898. <https://doi.org/10.13005/ojc/3404025>
- [7]. Altemimi, A., Lakhssassi, N., Baharlouei, A., Watson, D. G., & Lightfoot, D. A. (2017). Phytochemicals: Extraction, isolation, and identification of bioactive compounds from plant extracts. *Plants*, 6(4), 42. <https://doi.org/10.3390/plants6040042>
- [8]. Archana, E. (2020). Phytochemical analysis, bioactivity screening and characterization of biosynthesized silver nanoparticles on selected species of *Aglaia louriero* (Meliaceae) [Doctoral dissertation, University of Calicut]. <https://doi.org/10.14738/dafs.113.14904>
- [9]. Aslam, M., Ahmad, F., Khan, A., & Rasool, M. (2021). Phyto-extract-mediated synthesis of silver nanoparticles using aqueous extract of *Sanvitalia procumbens*: Characterization, optimization, and photocatalytic degradation of azo dyes Orange G and Direct Blue-15. *Molecules*, 26(20), 6144. <https://doi.org/10.3390/molecules2620614>
- [10]. Archana, E. (2020). Phytochemical analysis, bioactivity screening and characterization of biosynthesized silver nanoparticles on selected species of *Aglaia louriero* (Meliaceae) [Doctoral dissertation, University of Calicut].

- <https://doi.org/10.14738/dafs.113.14904>
- [11]. Aslam, M., Ahmad, F., Khan, A., & Rasool, M. (2021). Phyto-extract-mediated synthesis of silver nanoparticles using aqueous extract of *Sanvitalia procumbens*: Characterization, optimization, and photocatalytic degradation of azo dyes Orange G and Direct Blue-15. *Molecules*, 26(20), 6144. <https://doi.org/10.3390/molecules26206144>
- [12]. Baliyan, S., Sharma, A., Kumar, P., & Kumar, A. (2022). Determination of antioxidants by DPPH radical scavenging activity and quantitative phytochemical analysis of *Ficus religiosa*. *Molecules*, 27(4), 1326. <https://doi.org/10.3390/molecules27041326>
- [13]. Benjamaa, R., Moujanni, A., Choi, E. H., Essamadi, A. K., & Kaushik, N. K. (2022). Euphorbia species latex: A comprehensive review on phytochemistry and biological activities. *Frontiers in Plant Science*, 13, 1008881. <https://doi.org/10.3389/fpls.2022.1008881>
- [14]. Benjamaa, R., Moujanni, A., Kaushik, N., & Kaushik, N. K. (2024). Comparative evaluation of antioxidant activity, total phenolic content, anti-inflammatory, and antibacterial potential of Euphorbia-derived functional products. *Frontiers in Pharmacology*, 15, 1345340.
- [15]. Bharathi, S. V., & Das, M. (2022). Cytotoxicity effect of nanoparticles of Euphorbia antiquorum on breast cancer cell line. *South African Journal of Botany*, 151, 410–416. <https://doi.org/10.1016/j.sajb.2022.10.017>
- [16]. Bhardwaj, N., Goel, B., Tripathi, N., Sahu, B., & Jain, S. K. (2022). A comprehensive review on chemistry and pharmacology of marine bioactives as antimetastatic agents. *European Journal of Medicinal Chemistry Reports*, 4, 100023. <https://doi.org/10.1016/j.ejmcr.2021.100023>
- [17]. Che, H., et al. (2024). Ultrasound-assisted extraction of polyphenols from *Phyllanthi Fructus*: Comprehensive insights from extraction optimization and antioxidant activity. *Ultrasonics Sonochemistry*, 111, 107083. <https://doi.org/10.1016/j.ultsonch.2024.107083>
- [18]. Cömert, E. D., & Gökmen, V. (2017). Antioxidants bound to an insoluble food matrix: Their analysis, regeneration behavior, and physiological importance. *Comprehensive Reviews in Food Science and Food Safety*, 16(3), 382–399. <https://doi.org/10.1111/1541-4337.12263>
- [19]. Crisan, C. M., Mocan, T., Manolea, M., Lasca, L. I., Tabaran, F. A., & Mocan, L. (2021). Review on silver nanoparticles as a novel class of antibacterial solutions. *Applied Sciences*, 11(3), 1120. <https://doi.org/10.3390/app11031120>
- [20]. Dalimunthe, A., Yusuf, M., Sari, N., & Mahendra, D. (2024). In-depth analysis of lupeol: Delving into the diverse pharmacological profile. *Frontiers in Pharmacology*, 15, 1461478. <https://doi.org/10.3389/fphar.2024.1461478>
- [21]. Das, J., Das, M. P., & Velusamy, P. (2013). *Sesbania grandiflora* leaf extract mediated green synthesis of antibacterial silver nanoparticles against selected human pathogens. *Spectrochimica Acta Part A: Molecular and Biomolecular Spectroscopy*, 104, 265–270. <https://doi.org/10.1016/j.saa.2012.11.075>
- [22]. Di, G., Li-Tao, Y., Yao, S., & Zhi-Da, M. (2015). Structure and antibacterial property of a new diterpenoid from *Euphorbia helioscopia*. *Chinese Journal of Natural Medicines*, 13(9), 704–706. [https://doi.org/10.1016/s1875-5364\(15\)30069-8](https://doi.org/10.1016/s1875-5364(15)30069-8)
- [23]. Dikshit, P. K., Kumar, J., Das, A. K., & Singh, R. (2021). Green synthesis of metallic nanoparticles: Applications and limitations. *Catalysts*, 11(8), 902. <https://doi.org/10.3390/catal11080902>
- [24]. Dutta, G., Chinnaiyan, S. K., Sugumaran, A., & Narayanasamy, D. (2023). Sustainable bioactivity enhancement of ZnO–Ag nanoparticles in antimicrobial, antibiofilm, lung cancer, and photocatalytic applications. *RSC Advances*, 13(38), 26663–26682. <https://doi.org/10.1039/d3ra03736c>
- [25]. Elfeky, A. S., Ahmed, A. A., Hassan, A. M., & Ibrahim, M. A. (2020). Multifunctional cellulose nanocrystal/metal oxide hybrid: Photodegradation, antibacterial, and larvicidal activities. *Carbohydrate Polymers*, 230, 115711. <https://doi.org/10.1016/j.carbpol.2019.115711>
- [26]. El-Sayed, M. M., Hassan, A. A., & Salem, R. M. (2024). Selenium nanoparticles from *Euphorbia retusa* extract and its biological applications: Antioxidant and antimicrobial activities. *Egyptian Journal of Chemistry*, 67(2), 463–472. <https://doi.org/10.21608/ejchem.2023.214819.8069>
- [27]. Farooqi, M. A., Ahmad, N., Rahman, F., & Khan, S. (2024). Eco-friendly synthesis of bioactive silver nanoparticles from black roasted gram (*Cicer arietinum*) for biomedical applications. *Scientific Reports*, 14(1), 22922. <https://doi.org/10.1038/s41598-024-72356-5>
- [28]. Foti, M. C. (2015). Use and abuse of the DPPH radical. *Journal of Agricultural and Food Chemistry*, 63(40), 8765–8776. <https://doi.org/10.1021/acs.jafc.5b03839>
- [29]. Geetha, M., Nagabushana, H., & Shivananjaiiah, H. (2016). Green mediated synthesis and characterization of ZnO nanoparticles using *Euphorbia jatropha* latex as reducing agent. *Journal of Science: Advanced Materials and Devices*, 1(3), 301–310. <https://doi.org/10.1016/j.jsamd.2016.06.015>

- [30]. Ghasemi, S., Asadi, F., & Azizi, M. (2024). Process optimization for green synthesis of silver nanoparticles using *Rubus discolor* leaves extract and its biological activities against multi-drug resistant bacteria and cancer cells. *Scientific Reports*, 14(1), 4130. <https://doi.org/10.1038/s41598-024-54702-9>
- [31]. Gharanfoli, A., Mahmoudi, E., Torabizadeh, R., Katirae, F., & Faraji, S. (2019). Isolation, characterization, and molecular identification of *Candida* species from urinary tract infections. *Current Medical Mycology*, 5(2), 33–36. <https://doi.org/10.18502/cmm.5.2.1159>
- [32]. Gharpure, S., Yadwade, R., & Ankanwar, B. (2022). Non-antimicrobial and non-anticancer properties of ZnO nanoparticles biosynthesized using different plant parts of *Bixa orellana*. *ACS Omega*, 7(2), 1914–1933. <https://doi.org/10.1021/acsomega.1c05324>
- [33]. Horn, J. W., et al. (2012). Phylogenetics and the evolution of major structural characters in the giant genus *Euphorbia* L. (Euphorbiaceae). *Molecular Phylogenetics and Evolution*, 63(2), 305–326. <https://doi.org/10.1016/j.ympev.2011.12.022>
- [34]. Hadi, E. S., & Jasim, K. K. (2025). Role of Ag/ZnO nanoparticles for removal of pollutants from aqueous solutions: Characterization and environmental applications. *Journal of Nanostructures*, 15(1), 32–42. [https://jns.kashanu.ac.ir/article\\_114713.html](https://jns.kashanu.ac.ir/article_114713.html)
- [35]. Hussain, S., Awan, T. H., Waraich, E. A., & Awan, M. I. (2023). Plant abiotic stress responses and tolerance mechanisms. *In IntechOpen*. <https://doi.org/10.5772/intechopen.102138>
- [36]. Jalal, R., Goharshadi, E. K., Abareshi, M., Moosavi, M., Yousefi, A., & Nancarrow, P. (2010). ZnO nanofluids: Green synthesis, characterization, and antibacterial activity. *Materials Chemistry and Physics*, 121(1–2), 198–201. <https://doi.org/10.1016/j.matchemphys.2010.01.020>
- [37]. Joudeh, N., & Linke, D. (2022). Nanoparticle classification, physicochemical properties, characterization, and applications: A comprehensive review for biologists. *Journal of Nanobiotechnology*, 20(1), 262. <https://doi.org/10.1186/s12951-022-01477-8>
- [38]. Joshi, A. S., Singh, P., & Mijakovic, I. (2020). Interactions of gold and silver nanoparticles with bacterial biofilms: Molecular interactions behind inhibition and resistance. *International Journal of Molecular Sciences*, 21(20), 7658. <https://doi.org/10.3390/ijms21207658>
- [39]. Kemboi, D., Peter, X., Langat, M., & Tembu, J. (2020). A review of the ethnomedicinal uses, biological activities, and triterpenoids of *Euphorbia* species. *Molecules*, 25(17), 4019. <https://doi.org/10.3390/molecules25174019>
- [40]. Kokila, T., Ramesh, P., & Geetha, D. (2015). Biosynthesis of silver nanoparticles from Cavendish banana peel extract and its antibacterial and free radical scavenging assay: A novel biological approach. *Applied Nanoscience*, 5, 911–920. <https://doi.org/10.1007/s13204-015-0401-2>
- [41]. Lara, H. H., Romero-Urbina, D. G., Pierce, C., Lopez-Ribot, J. L., Arellano-Jiménez, M. J., & Jose-Yacaman, M. (2015). Effect of silver nanoparticles on *Candida albicans* biofilms: An ultrastructural study. *Journal of Nanobiotechnology*, 13, 1–12. <https://doi.org/10.1186/s12951-015-0147-8>
- [42]. Loo, Y. Y., Rukayadi, Y., Nor-Khaizura, M. A. R., & Kuan, C. H. (2018). In vitro antimicrobial activity of green synthesized silver nanoparticles against selected Gram-negative foodborne pathogens. *Frontiers in Microbiology*, 9, 1555. <https://doi.org/10.3389/fmicb.2018.01555>
- [43]. Mohamed, M. Y. A., Ferjani, H., Ogunjinmi, O. E., Jalouli, M., & Onwudiwe, D. C. (2024). Phyto-mediated synthesis of Ag, ZnO, and Ag/ZnO nanoparticles from leaf extract of *Solanum macrocarpon*: Evaluation of their antioxidant and anticancer activities. *Inorganica Chimica Acta*, 569, 122086. <https://doi.org/10.1016/j.ica.2024.122086>
- [44]. Monteiro, D. R., Gorup, L. F., Takamiya, A. S., & Camargo, E. R. (2015). Susceptibility of *Candida albicans* and *Candida glabrata* biofilms to silver nanoparticles in intermediate and mature development phases. *Journal of Prosthodontic Research*, 59(1), 42–48. <https://doi.org/10.1016/j.jpdr.2014.07.004>
- [45]. Nagaraja, S. K., Nayaka, S., & Kumar, R. S. (2023). Phytochemical analysis, GC–MS profiling, and in vitro evaluation of biological applications of different solvent extracts of *Leonotis nepetifolia* (L.) R.Br. flower buds. *Applied Biochemistry and Biotechnology*, 195(2), 1197–1215. <https://doi.org/10.1007/s12010-022-04201-2>
- [46]. Naqvi, Q. A., Ahmad, S., Khan, T., & Raza, M. (2019). Size-dependent inhibition of bacterial growth by chemically engineered spherical ZnO nanoparticles. *Journal of Biological Physics*, 45, 147–159. <https://doi.org/10.1007/s10867-019-9520-4>
- [47]. Pachaiappan, R., Rajendran, S., Show, P. L., Manavalan, K., & Naushad, M. (2021). Metal/metal oxide nanocomposites for bactericidal effect: A review. *Chemosphere*, 272, 128607. <https://doi.org/10.1016/j.chemosphere.2020.128607>
- [47]. Pawar, O., Deshpande, N., Dagade, S., Waghmode, S., & Joshi, P. N. (2016). Green synthesis of silver nanoparticles from purple acid phosphatase apoenzyme isolated from a new source *Limonia acidissima*. *Journal*

- of *Experimental Nanoscience*, 11(1), 28–37. <https://doi.org/10.1080/17458080.2015.1025300>
- [48]. Pascal, O. A., Bertrand, A. E. V., Esaïe, T., Sylvie, H.-A. M., & Eloi, A. Y. (2017). A review of the ethnomedical uses, phytochemistry, and pharmacology of the *Euphorbia* genus. *The Pharma Innovation*, 6(1 Part A), 34. <https://doi.org/10.1007/s11101-015-9449-6>
- [49]. Priya, C. L., & Rao, K. V. B. (2016). A review of phytochemical and pharmacological profile of *Euphorbia tirucalli*. *Pharmacologyonline*, 2, 384–390. <https://doi.org/10.9734/jabb/2016/26727>
- [50]. Raghupathi, K. R., Koodali, R. T., & Manna, A. C. (2011). Size-dependent bacterial growth inhibition and mechanism of antibacterial activity of zinc oxide nanoparticles. *Langmuir*, 27(7), 4020–4028. <https://doi.org/10.1021/la104825u><https://doi.org/10.3390/ijms21207658>
- [51]. Rajendran, N. K., George, B. P., Houreld, N. N., & Abrahamse, H. (2021). Synthesis of zinc oxide nanoparticles using *Rubus fairholmianus* root extract and their activity against pathogenic bacteria. *Molecules*, 26(10), 3029. <https://doi.org/10.1016/j.sajb.2022.10.017>
- [52]. Salem, W., Ezzat, S. M., Attia, A., Al-Qahtani, A., & Al-Ghamdi, A. (2015). Antibacterial activity of silver and zinc nanoparticles against *Vibrio cholerae* and enterotoxigenic *Escherichia coli*. *International Journal of Medical Microbiology*, 305(1), 85–95. <https://doi.org/10.1016/j.ijmm.2014.11.005>
- [53]. Saranraj, P., & Sujitha, D. (2015). Mangrove medicinal plants: A review. *American-Eurasian Journal of Toxicological Sciences*, 7(3), 146–156. <https://doi.org/10.29252/jmp.3.71.67>
- [54]. Sorbiun, M., Shayegan Mehr, E., Ramazani, A., & Taghavi Fardood, S. (2018). Biosynthesis of Ag, ZnO and bimetallic Ag/ZnO alloy nanoparticles by aqueous extract of oak fruit hull (Jaft) and investigation of photocatalytic activity of ZnO and bimetallic Ag/ZnO for degradation of basic violet 3 dye. *Journal of Materials Science: Materials in Electronics*, 29, 2806–2814. <https://doi.org/10.1007/s10854-017-8209-3>
- [55]. Sudha, T. S., & Padmini, R. (2023). Evaluation of bioactive compounds in *Euphorbia hirta* Linn. leaves extract using gas chromatographic and mass spectroscopic techniques. *Journal of Pharmaceutical Negative Results*, 14, 1. Retrieved November 22, 2025, from <https://www.pnrjournal.com/index.php/home/article/view/7858>
- [56]. Swathy, J., Sankar, M. U., Chaudhary, A., Aigal, S., Anshup, & Pradeep, T. (2014). Antimicrobial silver: An unprecedented anion effect. *Scientific Reports*, 4(1), 7161. <https://doi.org/10.1038/srep07161>
- [57]. Vasas, A., & Hohmann, J. (2014). *Euphorbia* diterpenes: Isolation, structure, biological activity, and synthesis (2008–2012). *Chemical Reviews*, 114(17), 8579–8612. <https://doi.org/10.1021/cr400541j>
- [58]. Vasas, A., & Hohmann, J. (2014). *Euphorbia* diterpenes: Isolation, structure, biological activity, and synthesis (2008–2012). *Chemical Reviews*, 114(17), 8579–8612. <https://doi.org/10.1021/cr400541j>
- [59]. Zare, M., Ghaedi, M., Gharibi, S., & Yousefi, A. (2019). Novel green biomimetic approach for synthesis of ZnO–Ag nanocomposite; Antimicrobial activity against food-borne pathogen, biocompatibility and solar photocatalysis. *Scientific Reports*, 9(1), 8303. <https://doi.org/10.1038/s41598-019-44309-w>
- [60]. El-Sayed, M. M., Hassan, A. A., & Salem, R. M. (2024). Selenium nanoparticles from *Euphorbia retusa* extract and its biological applications: Antioxidant and antimicrobial activities. *Egyptian Journal of Chemistry*, 67(2), 463–472. <https://doi.org/10.21608/ejchem.2023.214819.8069>
- [61]. Farooqi, M. A., Ahmad, N., Rahman, F., & Khan, S. (2024). Eco-friendly synthesis of bioactive silver nanoparticles from black roasted gram (*Cicer arietinum*) for biomedical applications. *Scientific Reports*, 14(1), 22922. <https://doi.org/10.1038/s41598-024-72356-5>
- [62]. oti, M. C. (2015). Use and abuse of the DPPH radical. *Journal of Agricultural and Food Chemistry*, 63(40), 8765–8776. <https://doi.org/10.1021/acs.jafc.5b03839>
- [63]. Ghasemi, S., Asadi, F., & Azizi, M. (2024). Process optimization for green synthesis of silver nanoparticles using *Rubus discolor* leaves extract and its biological activities against multi-drug resistant bacteria and cancer cells. *Scientific Reports*, 14(1), 4130. <https://doi.org/10.1038/s41598-024-54702-9>

## الخصائص المضادة للميكروبات والمضادة للأكسدة للجسيمات النانوية المصنعة من مستخلص نبات *Euphorbia spp* في إقليم كردستان العراق

شورش مصطفى عبدالله<sup>1</sup>روژيا عبدالجليل ناصر<sup>1</sup>

تقسم علوم الحياة، كلية العلوم، جامعة سوران.

### الخلاصة

أجريت هذه الدراسة بهدف تحليل في مكونات المستقلبات الثانوية لنباتات *Euphorbia Spp* الذي جُمع من منطقة سوران، في محافظة أربيل - العراق إضافة إلى تقييم قدرة مستخلصها المائي على تخليق جسيمات الفضة النانوية (*AgNPs*) وأكسيد الزنك النانوية (*ZnONPs*) ودراسة خصائصها المضادة للميكروبات ومضادات الأكسدة. تم تحليل التركيب الكيميائي النباتي لمستخلص النبات باستخدام تقنية *GC-MS*، بينما تم تأكيد تكوين الجسيمات النانوية المُحضَّرة باستخدام مجموعة من تقنيات التشخيص المتقدمة بما في ذلك *FTIR* و *XRD* و *SEM*. *EDS* لتقييم النشاط المضاد للبكتيريا والفطريات، تم تطبيق طريقة (*Diffusion Method*) *Well* كما تم استخدام اختبار *DPPH* كشف تحليل *GC-MS* عن وجود ثلاثة وعشرين مركبًا نباتيًا ثانويًا، وكانت المركبات الرئيسية إلى مجموعة ال(*triterpenoid*)، بما في ذلك *lanosterol* و *lupeol* و *taraxasterol* بالإضافة إلى مركبات أخرى من مجموعات مختلفة مثل ال *Alkaloids* وال *Phenols* وجد ان هذه المركبات لحيوية تلعب دورًا أساسيًا كعوامل مختزلة ومثبتة خلال عملية التخليق الأخضر، مما يساهم في التحكم بحجم الجسيمات وتحسين استقرارها البنيوي. أظهرت نتائج *SEM* و *XRD* وأن جسيمات الفضة النانوية تمتاز بشكل كروي منتظم ودرجة عالية من التبلور، بينما أظهرت جسيمات أكسيد الزنك النانوية بعض التكتل وتفاوتًا في الشكل البنيوي وفيما يتعلق بالنشاط المضاد للميكروبات، أثبتت جسيمات الفضة النانوية فعالية أعلى ضد السلالات البكتيرية والفطرية مقارنة بجسيمات أكسيد الزنك النانوية والمستخلص النباتي. كما أظهر اختبار *DPPH* لمستخلص نبات *Euphorbia* نشاطًا قويًا مضادًا للأكسدة، خاصةً عند التركيزات العالية. توضح هذه الدراسة طريقة خضراء مستدامة وناجحة لتخليق جسيمات نانوية نشطة بيولوجيًا، مع التأكيد في الوقت نفسه على أنواع *Euphorbia* مصدر طبيعي واعد لمركبات مضادة للأكسدة ومضاد للميكروبات قابلة للتطبيق في المجالات الصيدلانية والطب الحيوي.

الكلمات المفتاحية: *Euphorbia Spp*، التتميط الكيميائي النباتي، التخليق الأخضر، جسيمات الفضة والزنك النانوية، النشاط المضاد للميكروبات، النشاط المضاد للأكسدة.